Viscoplastic properties of chromium-nickel steel in short-term creep under constant stress. Part 1.

A. Yu. Kuzkin*, *Cand. Eng., Associate Prof., Dept. of Mechanical Engineering* [1]*, e-mail: Kuzkin_AYu@pers.spmi.ru;*
D. A. Zadkov, *Cand. Eng., Associate Prof., Dept. of Mechanical Engineering* [1]*, e-mail: Zadkov_DA@pers.spmi.ru;*
V. Yu. Skeeba, *Cand. Eng., Associate Prof., Dept. of Industrial Machinery Design* [2]*, e-mail: skeeba_vadim@mail.ru;*
V. V. Kukartsev, *Cand. Eng., Associate Prof., Dept. of Information Economic Systems, Institute of Engineering and Economics* [3]*, Dept. of Software Engineering, Institute of Space and Information Technologies* [4]*, Artificial Intelligence Technology Scientific and Education Center* [5]*, e-mail: vlad_saa_2000@mail.ru;*
Ya. A. Tynchenko, *Junior Researcher, Lab. of Biofuel Compositions* [4]*, Artificial Intelligence Technology Scientific and Education Center* [5]*, e-mail: t080801@yandex.ru*

[1] *Empress Catherine II Saint Petersburg Mining University (Saint Petersburg, Russia)*
[2] *Novosibirsk State Technical University (Novosibirsk, Russia)*
[3] *Reshetnev Siberian State University of Science and Technology (Krasnoyarsk, Russia)*
[4] *Siberian Federal University (Krasnoyarsk, Russia)*
[5] *Bauman Moscow State Technical University (Moscow, Russia)*
** Corresponding author, Kuzkin_AYu@pers.spmi.ru*

Mechanical processing of Chromium-nickel steel machining (cutting, pressure treatment) is impossible without taking into account their short-term creep and ductility properties. The purpose of this work is to study the formation and deformation development under short-term creep and constant effective stresses. The results of experimental tests of chromium-nickel steel 12Kh18N10T for short-term creep at room temperature are presented. A distinctive feature of the tests is the short-term creep in a wide range of stresses study: from the initial creep limit to the material destruction. The experiments were carried out under conditions of a stepwise increasing load (liquid pressure in a closed pipe) at a constant intensity of true stresses at each stage. It is shown that the conditions for changing the load, which ensure the constancy of the stress intensity, are violated at a sufficiently high voltage. Methods for separating the deformation into a plastic component and a component from short-term creep are proposed, which can be used both under conditions of stepped loading and under continuous loading. Examples of the occurrence and deformation development during short-term creep under conditions of decreasing stress are given.
Key words: short-term creep; viscous deformation; incrementally increasing load; creep at constant effective stress; viscoplastic deformation.
DOI: 10.17580/cisisr.2024.01.11

Introduction

The viscoplastic properties of chromium-nickel steels have a significant impact both on the process of manufacturing parts from these materials and on the properties of products made from them due to their high toughness and ductility [1–3]. Quite a large number of works have been devoted to the study of the viscoplastic properties of such steels. However, the range of issues studied in these works is quite wide. These are plastic properties, high-temperature plastic properties, and short-term creep. An important direction among these issues is the study of the interaction between the creep and plasticity [4–6], but the number of scientific papers devoted to these topics is currently limited. At the same time, taking into account these properties in the manufacture and operation of parts is extremely important [7–9].

Understanding the creep process is important in the under pressure operation of thin-walled parts, when high pressure acting on a thin-walled product made of plastic material contributes to the creep phenomenon formation [10–12]. Understanding the laws and creep behavior knowledge allows you to calculate thin-walled parts under pressure operation time or other technological load. It should be noted that the formalization of this problem will make it possible to understand under what operational loads the creep phenomenon will take place [13, 14]. In addition, experimental studies of viscoplastic properties are of interest for the development of viscoplastic materials theories and their empirical confirmation [15–17].

The authors show that the viscoplastic deformation at a high level of total inelastic deformation is comparable in magnitude to the instantaneous plastic deformation, so it should be taken into account in some metal forming technologies [18–20]. At the same time, the dependence of the viscoplastic component on the total inelastic deformation at small deformations in the range of 0.002–0.25 does not depend on the type of stress state of the material [21, 22]. When studying creep, it is necessary to take into account the complex stress state, because it is most often encountered in practice. Authors of [23, 24] show that when assessing creep damage and taking into account the complex stress state in the model to the material gives greater accuracy

Table 1. **The chemical composition of the 12H18N10T chromium-nickel steel used in this work (mass, %)**

C	Si	Cu	Mn	Ni	Ti	P	Cr	S
0.11	0.8	0.3	2.0	10.0	0.7	0.035	18.1	0.015

in comparison with the uniaxial model. Similarly, it is noted in [25, 26] that, in the case of biaxial and triaxial stress states, a different creep pattern is observed in the sample material. During intermittent tests, the voids formation at the grain boundaries is observed. It is shown that creep makes a significant contribution to the sample destruction process and affects its mechanical properties.

The works [27–30] among of the constant stress creep works. Its authors note that temporary effects (creep) take place at room temperature.

A study of the mechanical characteristics of steels with a high chromium content shows [31, 32], that the creep resistance is positively influenced by the high tungsten content. This is due to the separation of the Laves phase for chromium steels with the addition of tungsten. However, the addition of tungsten at high temperatures (~ 600 °C) reduces the steel ductility. In addition, for the investigated chromium steels, the plasticity characteristics are unstable at a temperature of 650 °C for a time exceeding 10,000–30,000 hours. The reasons for this behavior are not given in the article. In works [33–35] the authors conducted a study of a large number of pipe samples. As a result of the studies carried out, it was recorded that during tests lasting less than 30,000 hours, a fairly ac-curate prediction of failure is possible. The authors also conducted a comparative analysis of the creep characteristics behavior for different materials. Exploring the process of deformed materials unloading in stress-strain coordinates the authors [36–38] showed that different materials have different behavior patterns. So for low-carbon steels, unloading follows a curvilinear law. For aluminum alloys (duralumins) the unloading follows a linear law. In works [39, 40] the authors carry out modeling of metal behavior at small deformations. The modeling results are verified experimentally by the authors. The small plastic deformation theory developed by the authors allows an asymptotic solutions under loading at a constant strain rate. A new measure of sensitivity to the strain rate is proposed, which is independent of the stress level. The authors determined empirically for nickel steels the value of the time to failure during testing under conditions of a complexly deformed state [41–44]. The authors noted that the issues discussed in the articles require additional research. A detailed analysis of the work is given in the reviews [45, 46].

The works related to the study of plastic behavior and plasticity characteristics of nickel alloys and nickel-containing steels showed that there are a number of issues that require clarification. An important issue in this case is understanding in which case creep is characterized by a viscoplastic component of deformation, and in which case it is viscous.

The purpose of this work is to investigate the process of plastic deformation and short-term creep of chromium-nickel steel at different levels of true stresses in the range from creep limit to material destruction and to determine the patterns of creep deformation using the data obtained.

Materials and Methods

Cylindrical tubular samples for short-term creep tests were cut from seamless seamless pipes made of 12Kh18N10T steel and belonging to the same production batch. When setting up the experiment, we used the statistical method of multifactorial planning [47, 48].

Sample dimensions are: outer diameter $d_{ex0} = 26.4$ mm; wall thickness $t_0 = 0.3$ mm; the difference in wall thickness does not exceed 0.01 mm; the working section sample length equal to its 7–8 diameters. The mechanical properties of the sample material according to the certification were $\sigma_{0.2} = 325$ MPa, $\delta = 45\%$, $\psi = 60\%$. The nominal composition of the 12Kh18N10T chromium-nickel steel used in this study is shown in **Table 1**.

An MP-2500M deadweight gauge was used for testing, (**Fig. 1**). The deadweight gauge was used to create internal pressure in a tubular sample until the sample was destroyed. The screw press of the gauge *5* makes it possible to change the pressure value in the sample smoothly and with high accuracy when it is loaded. As can be seen from Fig. 1, to control the pressure in the sample, an exemplary (increased accuracy) gauge *2* is installed in the left socket of the deadweight pressure gauge, and the test sample *6*, assembled with grippers, is installed in the right socket. Free access to the sample makes it easy to measure its diameter at any time of testing with a micrometer without removing the sample from the grips. During testing, the outer diameter of the sample was measured under pressure (when the sample was unloaded) after each subsequent stage of loading. Therefore, the influence of the elastic component on the indication of the value of plastic deformation and deformation from short-term creep was excluded. The axial component of deformation in the realized stress state (loading of a pipe with closed ends by internal pressure) is equal to zero. The wall thickness of the sample, corresponding to the measured outer diameter of the sample, was calculated from the condition of volume constancy.

The desired pressure value in sample *6* is obtained in two steps. At the first stage, with a hand pump *8* and opened valve *7*, the system is filled, and the pre-pressure is reached in the sample. After that, valve *7* closes, and the exact pressure is set by screw press *5*. Measuring column *3* is disconnected from the hydraulic system by valve *4* throughout the experiment.

The pressure in the sample is released by opening valve *1*.

The experiments were carried out at room temperature 20 °C.

Test samples were cut off in pairs from the central part of the pipe and were adjacent parts of the pipe. During testing, both samples were loaded with internal pressure until the stress exceeded the creep limit strength of the material, then

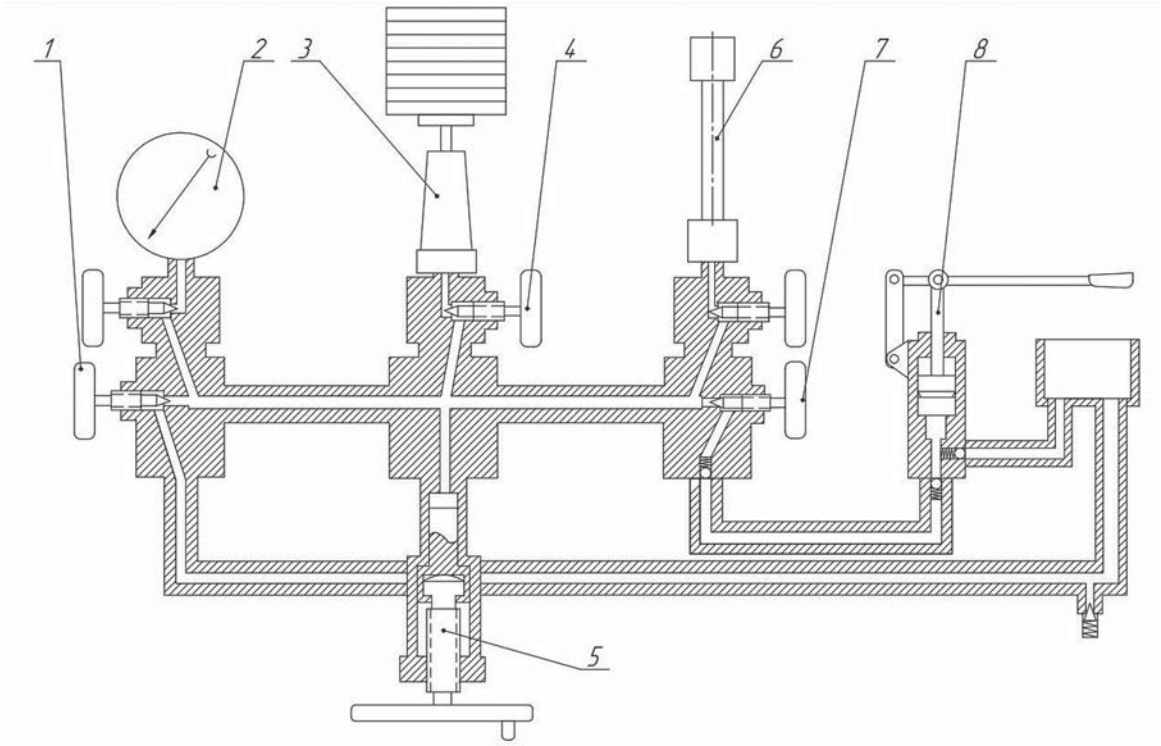

Fig. 1. Schematic diagram of the MP-2500M deadweigh gauge: *1* – drain valve; *2* – standard pressure gauge; *3* – measuring column with loads; *4* – measuring column check valve; *5* – screw press; *6* – test sample; *7* – hand pump check valve; *8* – hand pump.

they were loaded step-wise. The loading program made the same stress for each sample from the pair at each step as well as the same number of steps. The first sample from each pair was held under loading at each stage with a time delay of 1 s; the second sample from each pair was kept under load at each stage for 5 min. Step loading continued until the sample destroyed. The total number of steps during loading of one sample ranged from 18 to 25.

Results and Discussion

In the literature, sometimes ambiguous definitions of the deformation associated with the creep phenomenon are took place. Therefore, the definitions and hypotheses used in the article are given below. When describing the studies carried out, the definitions of "instantaneous plastic" and "viscous" deformations are understood as follows: viscous deformation is a deformation that develops over time at room (or elevated) temperature and constant stress [34]. Plastic deformation is a deformation that the sample obtains when the stress increases from raising the load between loading stages and holding it at the last stage for one s. Viscous deformation is the deformation that accumulates in the sample at the next stage of loading when holding it for five min. of constant stress. In this case, a step is a certain level of stress at which the sample is held for some time (in our experiment, this is 1 s and five min.). This time-exposure is done to study the viscous deformation buildup that accumulates from short-term creep. Comparison of the value sample material deformation value at each loading stage at an time-exposure of 1 s and an exposure of five min. will allow us to estimate the ratio of these deformations and determine the dependence of viscous deformation on the stress level in the material. Since "purely viscous" (hereinafter simply "viscous") deformation, as an independent component of inelastic deformation, does not actually occur, the main hypothesis about an elastoviscoplastic body [34] will be presented as follows:

$$\varepsilon_{ij} = \varepsilon_{ij}^{e} + \varepsilon_{ij}^{p} + \varepsilon_{ij}^{vp}, \quad (1)$$

where ε_{ij}^{e} and ε_{ij}^{p} are components of elastic and plastic deformations; ε_{ij}^{vp} are additive components containing viscous and plastic deformations.

The process of formation or accumulation of viscous (or viscoplastic) deformation will be defined as a creep behavior. For our purposes, it is rational to consider viscoplastic deformation as consisting of viscous and plastic components, which will allow us to estimate the ratio of these deformations and determine the dependence of viscous deformation on the stress level in the sample material.

A distinctive feature of the tests is the study of short-term creep in a wide range of stresses: from the creep limit to the destruction stress.

Formulas for finding stresses in the wall of a thin-walled tube were derived from the condition of a tube with closed ends and under internal pressure stressed state. In this case, the radial stress was taken equal to the average over the wall thickness, in which the radial stress on the outer side is equal to zero, and on the inner side it is equal to the pressure. The wall thickness small value allows us to consider the diagram of radial stress along the wall thickness as linear, while the

average stress is equal to half the pressure. For other stresses, the coefficient ½ appears when deriving formulas from the condition above.

Stresses in the sample are following – axial σ_z, ring σ_θ and radial σ_r correspond to the state of the pipe with closed ends, under the internal pressure p and were calculated by the formulas:

$$\sigma_z = p\frac{d_{ad}}{4t} - \frac{1}{2}p, \quad \sigma_\theta = p\frac{d_{ad}}{2t} - \frac{1}{2}p, \quad \sigma_r = -\frac{1}{2}p, \qquad (2)$$

where d_{ad} and t are current average diameter and sample wall thickness.

In the two-dimensional space of stress $\Sigma_1\Sigma_2$ by Prager-Ilushin

$$\Sigma_1 = \sigma_z - \frac{\sigma_\theta}{2} - \frac{\sigma_r}{2} \qquad \Sigma_2 = \frac{\sqrt{3}}{2}(\sigma_\theta - \sigma_r), \qquad (3)$$

The load path corresponding to stresses (2) will be determined:

$$\Sigma_1 = 0, \qquad \Sigma_2 = \frac{\sqrt{3}}{2}p\frac{d_{av}}{t}, \qquad (4)$$

In the corresponding strain space E_1E_2:

$$E_1 = 0, \quad E_2 = \frac{1}{\sqrt{3}}(\varepsilon_z + 2\varepsilon_\theta), \qquad (5)$$

The strain path is represented by the equations:

$$E_1 = 0 \qquad E_2 = \frac{2\varepsilon_\theta}{\sqrt{3}} \qquad \varepsilon_\theta = \ln\frac{d_{cd}}{d_{id0}}, \qquad (6)$$

where ε_θ is ring logarithmic deformation;

d_{cd}, d_{id0} are current and initial external diameters of the sample.

Thus, applying the parameters by Prager-Ilushin the universal values of strain and strain conditions are: streintensity $\bar{\sigma} = \sqrt{\Sigma_1^2 + \Sigma_2^2}$ and deformation intensity $\bar{\varepsilon} = \sqrt{E_1^2 + E_2^2}$ here are following:

$$\bar{\sigma} = \frac{\sqrt{3}}{4}p\frac{d_{av}}{t}, \qquad (7) \qquad \bar{\varepsilon} = \frac{2\varepsilon_\theta}{\sqrt{3}}. \qquad (8)$$

The functional dependencies for processing experimental data were obtained above while the experiment itself was carried out according to the procedure described in Section 2. Paired samples were selected from a series of products and tested on an experimental setup. One sample was subjected to loading with time-exposure at a step of 1 s, and the second sample – 5 min.

Paired samples deformed when the internal pressure increased in it. In this case, the entire range of stresses arising from pressure was divided into steps (stages) according to intermediate values.

The first sample, upon reaching the specified pressure at the stage, was held for one second, unloaded to measure the outer diameter and then loaded again up to the stress at the next stage, and so on. Based on the results of these tests, a deformation curve was built, or the so-called instantaneous load diagram $\bar{\sigma} = \bar{\sigma}(\bar{\varepsilon})$.

The second sample was loaded as follows:

1. Loading up to p_0 – pressure corresponding to a given stage, exposure for one second and unloading; d_0, t_0 are assumed to be initial sizes. The stress intensity calculated according to (7) is taken as the nominal

$$\bar{\sigma}_{pot} = \frac{\sqrt{3}}{4}p_0\frac{d_{ovd0}}{t_0}. \qquad (9)$$

2. Loading up to p_0 and reducing the pressure during the first minute to p_1 so that $\bar{\sigma}_{nom}$ kept unchanged, that is:

$$\bar{\sigma}_{pot} = \frac{\sqrt{3}}{4}p_1\frac{d_{ovd1}}{t_1}. \qquad (10)$$

From (9) and (10) with the account of $d_{ovd_1} = d_{ovd_0}e^{\varepsilon_{\theta 1}}$, $t_1 = t_0e^{\varepsilon_{r1}}$, and condition of volume stability (at $\varepsilon_z = 0$) $p_1 = p_0e^{-2\varepsilon_{\theta 1}}$.

Similar actions are carried out during every minute of the entire time period.

Thus, summarizing, we get

$$p_i = p_0e^{--2\varepsilon_{\theta i}}, \quad (i = 1, 2, \ldots, 5). \qquad (11)$$

So to keep $\bar{\sigma}$ constant, the pressure decrease according to (11).

It was previously mentioned that at each stage the stress intensity was kept constant for five minutes. Unloading after one minute is needed to control the deviation of the actual stress intensity from the nominal value.

Fig. 2*a* shows a diagram $\bar{\sigma}_T = \bar{\sigma}_T(\bar{\varepsilon}_T)$ of a creep tests at a single load stage with $\bar{\sigma} = \text{const}$, where $\bar{\sigma}_T$ and $\bar{\varepsilon}_T$ the intensity of stresses and deformations in the creep area "BC". The curve shows that at the flat area BC the stress is constant, while the deformation continues. As the diameter of the pipe changes because of the deformation, the pressure in pipe changes. The graph in **Fig. 2*b*** shows how the pressure in the sample must change during five minutes of holding on the stage in order for the stress intensity to remain constant ("BC" section in Fig. 2*a* to remain horizontal).

The number of such loading stages that the sample meet during testing before its destruction was 18–25. The total number of tested samples was more than fifty. **Fig. 3** shows samples before and after testing.

Fig. 4 shows the deformation diagrams of paired samples $\bar{\sigma} = \bar{\sigma}(\bar{\varepsilon})$. It is based on the test results of sample under instantaneous loading (T = 1 s at each stage); graph 2 – for a paired sample tested with a time delay T = 5 min (with $\bar{\sigma} = \text{const}$). The lines of unloading and subsequent loading to the initial pressure, are not shown here, as it was in Fig. 2*a*. **Table 2** shows part of the testing results thin-walled chromium-nickel steel tubes using a deadweight gauge. Loading was performed in steps, as described in section 2. Materials and Methods. The data are given for three stages of initial, intermediate and final, before the destruction of the sample.

The diagram $\bar{\sigma} = \bar{\sigma}(\bar{\varepsilon})$ instantaneous loading for the gap $0.074 \le \bar{\varepsilon} \le 0.307$ was approximated by a power law

$$\bar{\sigma} = 1480\bar{\varepsilon}^{0,4}, \qquad (12)$$

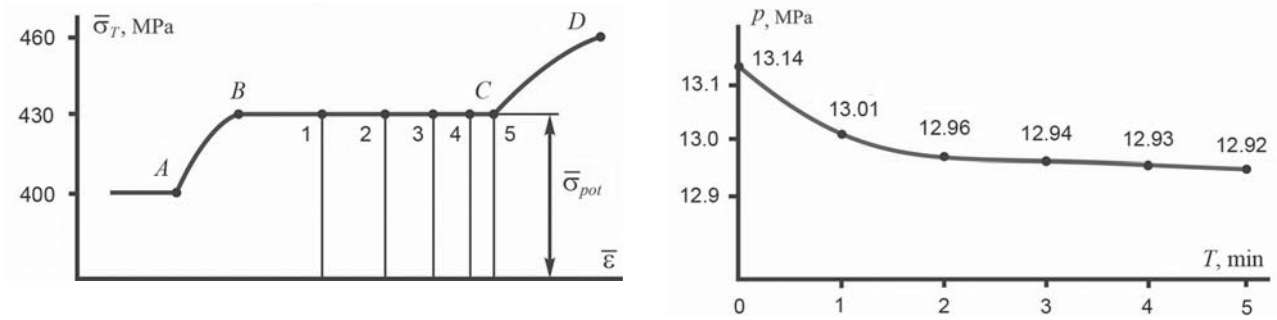

(*a*) (*b*)

Fig. 2. Creep test at $\bar{\sigma} = \text{const}$**:** *A* – end of the previous stage, *AB* – instantaneous loading to the next step, *BC* – creep state, where 1, 2, 3, 4, 5 – points characterizing the stress-strain state at the end of the 1st, ..., 5th minute, *C* – the end of the stage, *CD* – instantaneous loading to the next step (*a*); pressure change graph $p = p(T)$ on BC (*b*)

Which was used further to determine viscous deformation at significant deviations of the parts of the diagram $\bar{\sigma}_T(\bar{\varepsilon}_T)$ from the horizontal line.

The results of testing a paired sample with a change in pressure according to formula (12) for five minutes reveal that in the first ten to eleven steps the maximum deviations $\Delta\bar{\sigma}$ to $\bar{\sigma}_{\text{nom}}$ do not exceed 0,66 %. The graph parts $\bar{\sigma}_T = \bar{\sigma}_T(\bar{\varepsilon}_T)$ are horizontal, and they can be considered as representing creep states at $\bar{\sigma}_{\text{nom}} = \text{const}$. At subsequent steps, the creep areas (on the curve) acquire an increasing slope and a difference in the end and start points ordinates. Depending on the stress level at these steps, the deviations $\Delta\bar{\sigma}$ is equal to 1,23–3,42 % of $\bar{\sigma}_{\text{nom}}$.

Since viscous deformation does not cause hardening, the increment $\Delta\bar{\sigma}$ is due to the appearance of a plastic component of deformation, the value of which can be determined using the diagram of instantaneous loading of a paired sample. According to the diagram in **Fig. 5** viscoplastic deformation $\bar{\varepsilon}_k^{\text{vp}}$ on k$^{\text{th}}$ stage will be:

$$\bar{\varepsilon}_k^{\text{vp}} = \bar{\varepsilon}_k^{\text{in}} - \left(\bar{\varepsilon}_{k-1}^{\text{in}} + \bar{\varepsilon}_k^{p_{\text{mom}}}\right), \tag{13}$$

where $\bar{\varepsilon}_{k-1}^{\text{in}}$ and $\bar{\varepsilon}_k^{\text{in}}$ are anelastic deformation after the end of stages *k*-1and *k*, correspondingly; $\bar{\varepsilon}_k^{\text{pmom}}$ is momentum plastic deformation at transition onto *k*$^{\text{th}}$ stage.

With the help of (13) values of plastic deformation are determined at $\bar{\sigma} = \bar{\sigma}_{\text{nom}} + \Delta\bar{\sigma}_{\max}$ and $\bar{\sigma} = \bar{\sigma}_{\text{nom}}$. Their difference is a plastic component at the given stage is:

$$\bar{\varepsilon}_k^{p} = \bar{\varepsilon}_{|\bar{\sigma}=\bar{\sigma}}^{p} - \bar{\varepsilon}_{|\bar{\sigma}=\bar{\sigma}_{\text{nom}}}^{p} \tag{14}$$

The value of viscous deformation will be equal to:

$$\bar{\varepsilon}_k^{v} = \bar{\varepsilon}_k^{\text{vp}} - \bar{\varepsilon}_k^{p}. \tag{15}$$

(*a*) (*b*) (*c*)

Fig. 3. The samples with the clamping grapples before the test (*a*); coupled samples, where the left one is tested by the instantaneous load, and the right with 5 min time-exposure (*b*, *c*)

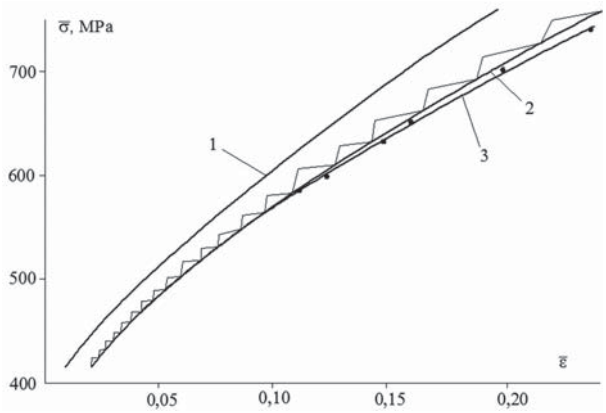

Fig. 4. Doubled samples deformation diagrams of: 1 – $\bar{\sigma} = \bar{\sigma}(\bar{\varepsilon})$ is instantaneous load (time-exposure $T = 1$ s at every stage); 2 – load at $\bar{\sigma}_T = \bar{\sigma}_T(\bar{\varepsilon}_T)$ $\bar{\sigma} = \text{const}$ with load change according to (12) during $T = 5$ min.; 3 – the specified graph $\bar{\sigma}_T = \bar{\sigma}_T(\bar{\varepsilon}_T)$, • are points of the specified graph).

Table 2. **The tested sample (d_{id_0}=26.28 mm, t_0=0.30 mm) experiment data. The time-exposure at every stage in creep conditions T = 5 min, $\bar{\sigma}$ = const**

Load stage number	T, s, min	p, MPa	d_{id}, mm	ε_θ	ε_r	t, mm	Σ_2, MPa	E_2	$\bar{\varepsilon}$	$\bar{\sigma}$, MPa
1	1 s	10.80	26.503	0.0084	–0.0084	0.2975	412.0	0.0098	0.0098	412.0
	1 min	10.77	26.593	0.0118	–0.0118	0.2965	413.5	0.0137	0.0137	413.5
	2 min	10.75	26.603	0.0122	–0.0122	0.2964	413.1	0.0141	0.0141	413.1
	3 min	10.74	26.610	0.0125	–0.0125	0.2963	413.0	0.0144	0.0144	413.0
	4 min	10.73	26.616	0.0127	–0.0127	0.2962	413.0	0.0147	0.0147	413.0
	5 min	10.72	26.621	0.0129	–0.0129	0.2962	413.1	0.0149	0.0149	413.1
										$\Delta\bar{\sigma}_{max} = 1.5$
13	1 s	13.00	28.520	0.0818	–0.0818	0.2764	575.1	0.0945	0.0945	575.1
	1 min	12.95	28.681	0.0874	–0.0874	0.2749	579.6	0.1010	0.1010	579.6
	2 min	12.93	28.750	0.0898	–0.0898	0.2742	581.3	0.1037	0.1037	581.3
	3 min	12.91	28.788	0.0911	–0.0911	0.2739	582.3	0.1053	0.1053	582.3
	4 min	12.91	28.818	0.0922	–0.0922	0.2736	583.2	0.1065	0.1065	583.2
	5 min	12.90	28.835	0.0928	–0.0928	0.2734	583.7	0.1071	0.1071	583.7
										$\Delta\bar{\sigma}_{max} = 8.6$
18	1 s	13.80	31.312	0.1752	–0.1752	0.2518	737.1	0.2023	0.2023	737.1
	1 min	13.65	31.863	0.1926	–0.1926	0.2474	755.0	0.2224	0.2224	755.0
	2 min	13.57	31.988	0.1965	–0.1965	0.2465	756.7	0.2270	0.2270	756.7
	3 min	13.53	32.057	0.1987	–0.1987	0.2459	757.6	0.2294	0.2294	757.6
	4 min	13.50	32.093	1.1998	–0.1998	0.2457	758.1	0.2307	0.2307	758.1
	5 min	13.49	32.121	0.2007	–0.2007	0.2454	758.8	0.2318	0.2318	758.8
										$\Delta\bar{\sigma}_{max} = 21.7$

Conclusion

The work carried out to study the plastic behavior and ductility characteristics of nickel steel 12Kh18N10T made it possible to clarify a number of issues. One of the important results of this work was the understanding in which case creep is characterized by a viscoplastic component of deformation, and in which by viscous one.

As a research result, the following conclusions have been established that the condition for maintaining a constant stress intensity (σ = const) at each loading step is observed up to the level of inelastic deformation $\bar{\varepsilon}_k^{in} = 7.0...7.5\%$. In this case, the creep deformation is represented only by the viscous component. At higher values $\bar{\varepsilon}_k^{in}$, possibly due to an increase in microdamages and a decrease in the effective cross-sectional area, an increase $\bar{\sigma}$, and the creep process is characterized by the viscoplastic deformation component.

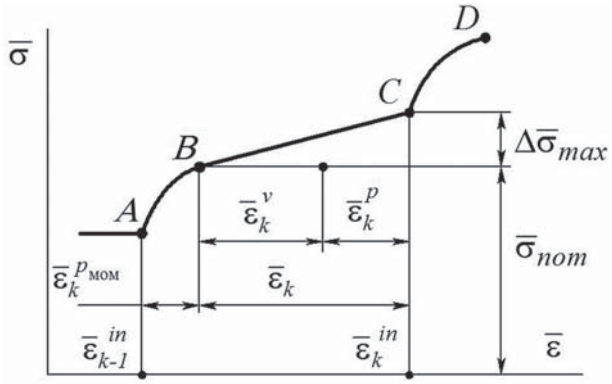

Fig. 5. Viscous deformation determination during deviation from $\bar{\sigma}$ = const

REFERENCES

1. Wurmbauer H., Panzenböck M., Leitner H., Scheu C., Clemens H. Short-term creep behavior of chromium rich hot-work tool steels. *Materialwissenschaft und Werkstofftechnik*. 2010. Vol. 41. No. 1. pp. 18–28. DOI: 10.1002/mawe.200900527.
2. Smirnov S. V., Zamaraev L. M., Matafonov P. P. Short-term creep in electrical-engineering steel. *Steel in Translation*. 2009. Vol. 39. No. 1. pp. 17. DOI: 10.3103/S0967091209010069.
3. Latyshev D., Mitukov A., Petrov M., Popov V. Viscoplastic properties of chromium-nickel steel at increasing and constant loads. *Journal of Engineering Science*. 2012. Vol. 2. No. 147. pp. 151–160.
4. Holdsworth S. Creep-Ductility of High Temperature Steels. *A Review Metals*. 2019. Vol. 9. No. 3. pp. 342. DOI: 10.3390/met9030342.
5. Skelton R. P. Deformation, diffusion and ductility during creep–continuous void nucleation and creep-fatigue damage. *Materials at High Temperatures*. 2017. Vol. 34. No. 2. pp. 121–133. DOI: 10.1080/09603409.2016.1252888.
6. Sandatrom R., Jun-Jing H. Prediction of creep ductility for austenitic stainless steels and copper. *Materials at High Temperatures*. 2022. Vol. 39. No. 1. pp. 1–9. DOI: 10.1080/09603409.2022.2039497.
7. Maksarov V. V., Keksin A. I., Filipenko I. A. Influence of magnetic-abrasive processing on roughness of flat products made of AMTs grade aluminum alloy. *Tsvetnye Metally*. 2022. No. 7. pp. 82–87.
8. Maksarov V. V., Popov M. A., Zakharova V. P. Influence of magnetic-abrasive machining parameters on ceramic cutting tools for technological quality assurance of precision products from cold-resistant steels. *Chernye Metally*. 2023. No. 1. pp. 67–73.
9. Olt Y. Y., Maksarov V. V., Efimov A. E. Improving the quality of the surface of products from titanium alloys in the process of machining. *STIN*. 2023. No. 1. pp. 26–30. DOI: 10.25960/mo.2022.5-6.41.

10. Milyuts V. G., Tsukanov V. V., Pryakhin E. I., Nikitina L. B. Development of Manufacturing Technology for High-Strength Hull Steel Reducing Production Cycle and Providing High-Quality Sheets. *Journal of Mining Institute*. 2019. Vol. 239. p. 536. DOI: 10.31897/pmi.2019.5.536.
11. Marinin M. A., Khokhlov S. V., Isheyskiy V. A. Modeling of the Welding Process of Flat Sheet Parts by an Explosion. *Journal of Mining Institute*. 2019. Vol. 237. p. 275. DOI: 10.31897/pmi.2019.3.275.
12. Bolobov V. I., Popov G. G. Methodology for testing pipeline steels for resistance to grooving corrosion. *Journal of Mining Institute*. 2021. Vol. 252. No. 6. pp. 854–860. DOI: 10.31897/PMI.2021.6.7.
13. Vologzhanina S., Igolkin A., Peregudov A., Baranov I., Martyushev N. Effect of the deformation degree at low temperatures on the phase transformations and properties of metastable austenitic steels. *Obrabotka Metallov*. 2022. Vol. 24. No. 1. pp. 73–86. DOI: 10.17212/1994-6309-2022-24.1-73-86.
14. Volokitina I., Siziakova E., Fediuk R., Kolesnikov A. Development of a thermomechanical treatment mode for stainless-steel rings. *Materials*. 2022. Vol. 15. No. 14. DOI: 10.3390/ma15144930.
15. Maksarov V. V., Keksin A. I., Filipenko I. A. Improvement of magnetic-abrasive finishing of nonuniform products made of high-speed steel in digital conditions. *Key Engineering Materials*. 2020. Vol. 834. pp. 71–77. DOI: 10.4028/www.scientific.net/KEM.836.71.
16. Bazhin V. Y., Issa B. Influence of heat treatment on the microstructure of steel coils of a heating tube furnace. *Journal of Mining Institute*. 2021. Vol. 249. No. 5. pp. 393–400. DOI: 10.31897/PMI.2021.3.8.
17. Pryakhin E. I., Sharapova D. M. Understanding the structure and properties of the heat affected zone in welds and model specimens of high-strength low-alloy steels after simulated heat cycles. *CIS Iron and Steel Review*. 2020. Vol. 19. pp. 60–65.
18. Kolebina N. V.. Danilov V. L., Prizan C. Investigation of short-term creep of prospective turbine steel. *Nauka I obrazovanie: nauchnoe izdanie MGTU im. Baumana*. Electronic journal. 2014. Vol. 11. DOI: 10.7463/1114.0733687.
19. Volkov I. A., Igumnov L. A., Kazakov D. A., Shishulin D. N., Smetanin I. V. Determining relations of unsteady creep in a complex stress state. *Problemy prochnosti i plastichnosti*. 2016. Vol. 78. No. 4. pp. 436–451. DOI: 10.32326/1814-9146-2016-78-4-436-451.
20. Bondar V. S., Abashev D. R., Fomin D. Y. Comparative analysis of plasticity theories undtr complex loading. *Problemy prochnosti i plastichnosti*. 2022. Vol. 84. No. 4. pp. 493–510. DOI: 10.32326/1814-9146-2022-84-4-493-510.
21. Nai Q. Z., Hong X., Xue P. M., Gang W. Study on high temperature creep behaviors of P92 steel. *Key Engineering Materials*. 2011. pp. 452–453. 521–524. DOI: 10.4028/www.scientific.net/KEM.452-453.521.
22. Woodford D. A. Intrinsic ductility for structural materials as a function of stress and temperature. *Mater. High Temp*. 2017. Vol. 34. pp. 134–139.
23. Itoh R., Hikida T., Ogawa F., Itoh T., Sakane M., Zhang S. Biaxial tensile creep damage of Mod.9Cr–1Mo steel using cruciform specimen. *Proceedings of 9th China–Japan Bilateral Symposium on High Temperature Strength of Materials*. 2016. pp. 60–66.
24. Kobayashi H., Ohki R., Itoh T., Sakane M. Multiaxial creep damage and lifetime evaluation under biaxial and triaxial stresses for type 304 stainless steel. *Engineering Fracture Mechanics*. 2017. Vol. 174. pp. 30–43. DOI: 10.1016/j.engfracmech.2017.01.001.
25. Sakane M., Kobayashi H., Ohki R., Itoh T. Creep void formation and rupture lifetime in multiaxial stress states. *Key Engineering Materials*. 2019. Vol. 795. pp. 159–164. DOI: 10.4028/www.scientific.net/KEM.795.159.
26. Karlina A. I., Kondratyev V. V., Kolosov A. D., Balanovskiy A. E., Ivanov N. A. Production of new nanostructures for modification of steels and cast irons. *IOP Conference Series: Materials Science and Engineering*. 2019. Vol. 560. No. 1. p. 012183.
27. John H. Creep Strength And Ductility of 9 to 12 % Chromium Steels. *Materials at High Temperatures*. 2004. Vol. 21. No. 1. pp. 41–46. DOI: 10.1179/mht.2004.006.
28. Wilshire B., Scharning P. Extrapolation of creep life data for 1Cr–0.5Mo steel. *International Journal of Pressure Vessels and Piping*. 2008. Vol. 85. No. 10. pp. 739–743. DOI: 10.1016/j.ijpvp.2008.04.002.
29. Wilshire B., Scharning P. Creep ductilities of 9–12 % chromium steels. *Scripta Materialia*. 2007. Vol. 56. No. 12. pp. 1023–1026. DOI: 10.1016/j.scriptamat.2007.03.003.
30. Zhukov A. Unloading of plastically deformed metals and sequential loading. *Byulleten AN SSSR. Mekhanika tverdykh tel*. 1989. Vol. 2. pp. 179–183.
31. Zhukov A. Non-ferrous metals and alloys creep at room temperature beyond elasticity. *Inzherenyi zhurnal*. 1963. Vol. 2. pp. 409–413.
32. Martyushev N. V., Kozlov V. N., Qi M., Tynchenko V. S., Kononenko R. V., Konyukhov V. Yu., Valuev D. V. Production of Work-pieces from Martensitic Stainless Steel Using Electron-Beam Surfacing and Investigation of Cutting Forces When Milling Workpieces. *Materials*. 2023. Vol. 16. pp. 4529. DOI: 10.3390/ma16134529.
33. Gomaa S., Sham T.-L., Krempl. E. Finite element formulation for finite deformation, isotropic viscoplasticity theory based on overstress (FVBO). *International Journal of Solids and Structures*. 2004. Vol. 41. No. 13. pp. 3607–3624.
34. Krempl E. Phenomenologigal Modelling of Viscoplasticity. *Rev. phys. appl*. 1988. Vol. 23. No. 4. pp. 331–338.
35. Giginyak F. F., Maslo O. M. A relationship between damage in 10GN2MFA steel and low-cycle strain-controlled loading at different deformation frequencies. *Strength of Materials*. 2017. Vol. 49. No. 2. pp. 343–348. DOI: 10.1007/s11223-017-9874-4.
36. Yelemessov K., Baskanbayeva D., Martyushev N. V., Skeeba V. Y., Gozbenko V. E., Karlina A. I. Change in the Properties of Rail Steels during Operation and Reutilization of Rails. *Metals*. 2023. Vol. 13. pp. 1043. DOI: 10.3390/met13061043.
37. Vasin R. Constitutive equations of plasticity theory. *Itogi nauki i techniki*. 1990. Vol. 21. pp. 3–75.
38. Semenov A., Melnikov B., Gorokhov M., Ulbricht V. Prevention of cyclic instability at the modeling of elasto-plastic deformation at large strains under proportional and non-proportional loading. *Proceedings of SPIE*. 2007. Vol. 6597. p. 659710.
39. Semenov A., Melnikov B., Gorokhov M. About the causes of cyclical instability at computations of large elasto-plastic strains. *Proceedings of SPIE*. 2005. Vol. 5831. pp. 167–173.
40. Knyazev S., Dmitrienko V., Gizatulin R., Martyushev N., Valuev D., Karlina A. Research for Replacement of Gray Cast Irons for Manufacturing Electrolyzer Gas Collection Bell Cast Components. *Metallurgist*. 2023. Vol. 66. No. 9–10. pp. 1201–1215. DOI: 10.1007/s11015-023-01433-3.
41. Novozhilov V., Kadashevich U. Microstrains in construction materials. Leningrad: Mashinostroenie. 1990. pp. 78–123.
42. Isametova M. E., Martyushev N. V., Karlina Yu. I., Kononenko R. V., Skeeba V. Y. , Absadykov B. N. Thermal Pulse Processing of Blanks of Small-Sized Parts Made of Beryllium Bronze and 29 NK Alloy. *Materials*. 2022. Vol. 15. pp. 6682. DOI: 10.3390/ma15196682.
43. Wang Y., Zhang W., Wang Y., Lim Y. C., Yu X., Feng Z. Experimental Evaluation of Localized Creep Deformation in Grade 91 Steel Weldments. *Materials Science and Engineering A*. 2021. Vol. 799. pp. 140356. DOI: 10.1016/j.msea.2020.140356.
44. Nguyen T. T., Jeong T. M., Erten D. T., Yoon K. B.Creep deformation and rupture behaviour of service-exposed super 304H steel boiler tubes. *Materials at High Temperatures*. 2021. Vol. 38. No. 1. pp. 61–72. DOI: 10.1080/09603409.2020.1830609.
45. Martyushev N. V., Bublik D. A., Kukartsev V. V., Tynchenko V. S., Klyuev R. V., Tynchenko Y. A., Karlina Yu. I. Provision of Rational Parameters for the Turning Mode of Small-Sized Parts Made of the 29 NK Alloy and Beryllium Bronze for Subsequent Thermal Pulse Deburring. *Materials*. 2023. Vol. 16. pp. 3490. DOI: 10.3390/ma16093490.
46. Cheng C. S. Theory of Factorial Design: Single- and Multi-Stratum Experiments. CRC Press. 2016. 409 p.
47. Zverev E., Skeeba V., Ivancivsky V., Vakhrushev N., Titova K., Lobanov D., Martyushev N. Determining the Residual Stresses in High-Chromium Cast Iron Plasma Coatings. *Key Engineering Materials*. 2022. Vol. 909. pp. 94–100. DOI: 10.4028/p-2a9z55.
48. Adigamov R. R., Baraboshkin K. A., Mishnev P. A., Karlina A. I. Development of rolling procedures for pipes of K55 strength class at the laboratorial mill. *CIS Iron and Steel Review*. 2022. Vol. 24. pp. 60–66.